Limitations of the Effective Mass Approximation: A Specific Example

Aniello Esposito[1] **and Andreas Schenk**[1,2]

[1] Integrated Systems Laboratory, ETH Zurich, Gloriastrasse 35, CH-8092, Switzerland,
(esposito@iis.ee.ethz.ch / schenk@iis.ee.ethz.ch)
[2] Synopsys LLC., Affolterstrasse 52, CH-8050 Zurich, Switzerland

Abstract

A suitable Schrödinger problem is solved by exact diagonalization (ED) and the result is compared to the one obtained via the effective mass approximation (EMA). The problem consists of an optical lattice embedded in a confining external potential (EP). By decreasing the EP width in the present case from ≈7nm down to ≈1nm the EMA is found to increasingly overestimate the ground state energy (GSE) in the regime below ≈2nm. For EP widths well above ≈2nm the EMA reproduces the GSE up to ≈1 meV.

1. Introduction

The progressive scaling of modern semiconductor devices down to the nanometer regime requires a full quantummechanical treatment (FQT) in order to be able to reliably predict interesting quantities such as currents or charge densities. As the computational burden related to the FQT drives the simulation time on a common workstation beyond reasonable limits some simplifications are required. A widely used simplification in nowadays semiconductor device simulators [1] is given by the effective mass approximation (EMA) [2]. However, the EMA as any other approximation is bound to some specific restrictions. The most important condition requires that the variation of an external perturbation is small compared to the lattice constant of the underlying semiconductor material. Investigations on the validity of the EMA in quantum transport calculations of silicon quantum wires have been reported [4]. In this work the groundstate properties of a confined optical lattice are considered in order to study the limitations of the EMA.

2. The Model

An optical lattice in three dimensions is given by the expression

$$V(\vec{r}) = V_0 \sum_{i=1}^{3} \sin^2\left(\frac{\pi x_i}{a}\right), \tag{1}$$

where V_0 denotes the amplitude and a the periodicity. The simulation box is delimited by $\Omega \equiv [-Na/2, Na/2]^3$ and the external potential (EP) reads

$$\widetilde{U}(\vec{r}) = U_0 \left(1 - \chi_b(\vec{r})\right), \tag{2}$$

where χ_b is unity on $[-Nb/2, Nb/2]^3$ and zero elsewhere. The length $d \equiv \sqrt{3}Nb$ is referred to as the EP width. In order to obtain a smooth confinement the potential $\widetilde{U}$ from Eq. (2) undergoes a convolution with a Gaussian mollifier

$$U(\vec{r}) \equiv \frac{1}{|\Omega|} \int_\Omega \widetilde{U}(\vec{r}')F_\epsilon(\vec{r} - \vec{r}')d\vec{r}' \tag{3}$$

$$F_\epsilon(\vec{r}) \equiv \sum_{\vec{v}\in\Lambda(\Omega)} \frac{|\Omega|}{(2\pi)^{3/2}\epsilon^3} \exp\left[-\frac{1}{2}\frac{(\vec{r} - \vec{v})^2}{\epsilon^2}\right], \tag{4}$$

where $\Lambda(\Omega) \equiv \{Na\vec{n} | \vec{n} \in \mathbb{Z}^3\}$. In the following

$$\{N = 15, a = 10a_B, \epsilon = 0.2a_B, U_0 = 4.1eV, V_0 = 0.5eV\} \tag{5}$$

with $a_B = 0.052$nm. The $V(\vec{r})$ as well as the $U(\vec{r})$ are illustrated in Fig. 1. The stationary Schrödinger equation is given by

$$\widehat{\mathbf{H}}\Psi = E\Psi \tag{6}$$

with Hamilton operators $\widehat{\mathbf{H}}$ for the two different approaches

$$\widehat{\mathbf{H}}^{\mathrm{ED}} \equiv -\frac{\hbar^2}{2m_e}\Delta + V(\vec{r}) + U(\vec{r}) \tag{7}$$

$$\widehat{\mathbf{H}}^{\mathrm{EMA}} \equiv -\frac{\hbar^2}{2m_e}\vec{\nabla}\mathbf{M}\vec{\nabla}^T + U(\vec{r}) + E_0, \tag{8}$$

where $\hbar$ is Planck's constant and m_e the free electron mass. The effective mass tensor $\mathbf{M}$ from Eq. (8) is given by the unit matrix divided by $m_0 = 1.006$ and the edge is $E_0 = 0.79$eV. The derivation of the EMA Hamiltonian $\widehat{\mathbf{H}}^{\mathrm{EMA}}$ from the full operator $\widehat{\mathbf{H}}^{\mathrm{ED}}$ is explained in detail in Ref. [2]. For a given external perturbation $U(\vec{r})$ the Schrödinger equation is solved by ED and via the EMA simultaneously and the resulting groundstate energies (GSE) as well as wavefunctions are compared to each other. The difference of the wavefunctions is computed by means of the $\mathbf{L}_2$ norm. Note that the wavefunctions resulting from Eq. (6) are normalized to unity on the simulation domain Ω according to

$$1 \stackrel{!}{=} \int_\Omega |\Psi|^2 d\vec{r}. \tag{9}$$

3. Solution

The Schrödinger equations resulting from the two Hamilton operators given in Eqs. (7) and (8) are solved by expanding the wavefunction $\Psi(\vec{r})$ in terms of planewaves

$$\Psi(\vec{r}) = \sum_{\vec{G}\in\Gamma(\Omega)} c(\vec{G}) \exp(i\vec{G}\vec{r}), \tag{10}$$

where $\Gamma(\Omega) \equiv \{2\pi\vec{n}/(Na) | \vec{n} \in \mathbb{Z}^3\}$. After inserting the ansatz from Eq. (10) in the problem given in Eq. (6) and integrating on both sides with $(1/|\Omega|)\int_\Omega \exp(-i\vec{G}'\vec{r})\ldots d\vec{r}$ the Hamilton operator becomes a Matrix

$$\mathbf{H}(\vec{G}', \vec{G}) = \frac{1}{|\Omega|}\int_\Omega \exp(-i\vec{G}'\vec{r})\widehat{\mathbf{H}}\exp(i\vec{G}\vec{r})d\vec{r}. \tag{11}$$

For numerical purposes a reduced set of planewaves

$$\widetilde{\Gamma}(\Omega) \equiv \{2\pi(n_1, n_2, n_3)/(Na) | n_1 = -M, \ldots, M \quad i = 1, 2, 3\} \tag{12}$$

is used. The resulting matrices are diagonalized on a Cray XT3 machine by means of the ScaLAPACK routine PDSYEVX as well as via an alternative diagonalization algorithm (RMDIIS [3]) being suitable for the plavewave expansion given in Eq. (10). Figure 2 illustrates the scaling behavior of both diagonalization methods as well as the time for the matrix assembly. The PDSYEVX routine shows a better scaling behavior compared to the RMDIIS method which on the other hand is found to be notably faster than the PDSYEVX routine.

The convergence properties of the groundstate energy (GSE) as well as the wave function differences depending on the size of $\widetilde{\Gamma}(\Omega)$ are shown in Fig. 3. Two limiting cases of a strong ($b = 1a_B$) and a weak ($b = 9a_B$) confinement are illustrated. In both cases the EMA GSE is found to converge faster than the ED GSE, where the convergence criterion is set to $1meV$. Note that for the strong confinement case up to 103823 planewaves, i.e. $M = 23$, are required for the wavefunction difference to converge. In the latter case the convergence criterion is set to $\approx 5\%$ of relative error. However, the investiagation of the EMA limitations in this work is focused on the GSE.

In the following the RMDIIS is the method of choice and $M = 23$. Furthermore a fix amount of 128 computing nodes is used because of memory purposes.

4. Results and Discussion

The EP width $d = \sqrt{3}Nb$ is ramped from $b = 9a_B$ down to $b = 1a_B$ and the resulting GSEs are plotted in Fig 4. Except of the region below ≈ 2nm the EMA is found to reproduce the ED GSEs satisfactorily well. The wavefunction difference in the case of the weakest and the strongest confinement differs by almost a factor of ten. As the effective mass $m_0 = 1.006$ is close to unity the amplitude V_0 is rather small compared to reality. This can possibly explain why the suitability range of the EMA in this work is larger than the one obtained in Ref. [4].

The procedure presented in this work is not bound to a specific case such as the optical lattice and can be easily modified in order to perform similar investigations in more realistic environments such as pseudopotentials subjected to external perturbations.

References

[1] F. O. Heinz and A. Schenk: *Self-consistent modeling of longitudinal quantum effects in nanoscale double-gate metal oxide semiconductor field effect transistors*, J. Appl. Phys., no. 100 (2006), 084314.

[2] J.M. Luttinger and W. Kohn: *Motion of Electrons and Holes in Perturbed Periodic Fields*, Phys. Rev., no. 97 (1954), 869–883.

[3] D.M. Wood and A. Zunger: *A new method for diagonalizing large matrices*, J. Phys. A: Math. Gen., no. 18 (1985), 1343–1359.

[4] J. Wang, A. Rahman, A. Gosh, G. Klimeck, and M. Lundstrom: *On the Validity of the Parabolic Effective-Mass Approximation for the I-V Calculation of Silicon Nanowire Transistors*, IEEE Transactions on Electron Devices, no. 52, 1589–1595.

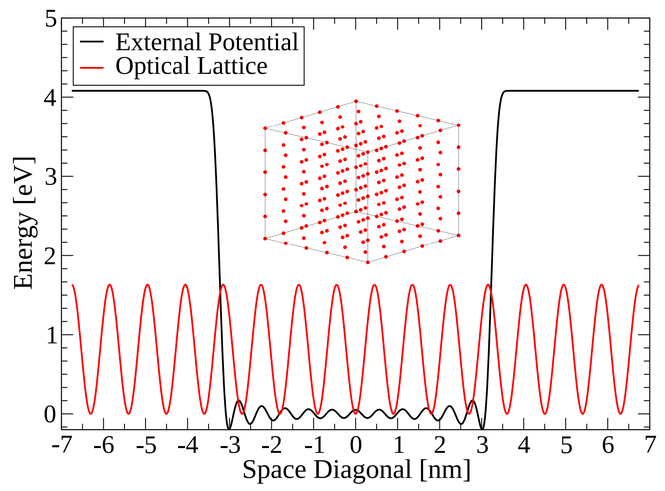

Figure 1: *$V(\vec{r})$ and $U(\vec{r})$ from Eqs. (1) and (3) for the parameters given in Eq. (5). Plotted is a cut along the space diagonal of Ω. The inset shows a schematic representation of the optical lattice in three dimensions.*

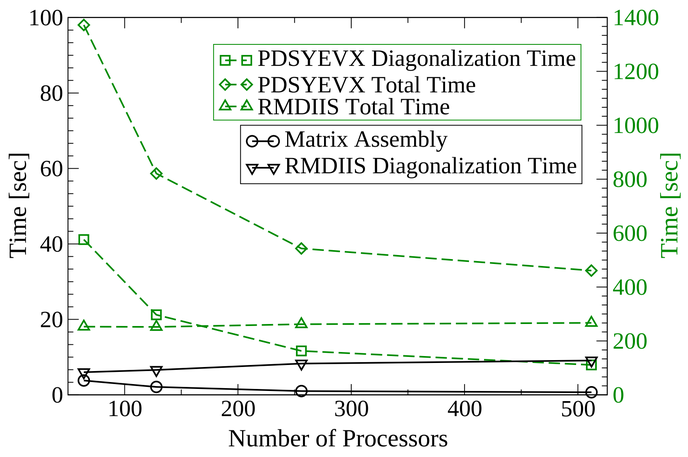

Figure 2: *Scaling properties of the diagonalization and assembly time. For this specific problem the RMDIIS method is significantly faster than the PDSYEVX routine. For the comparison the matrix size is set to 29791^2, i.e. $M = 15$. Note the affiliation to the corresponding ordinates.*

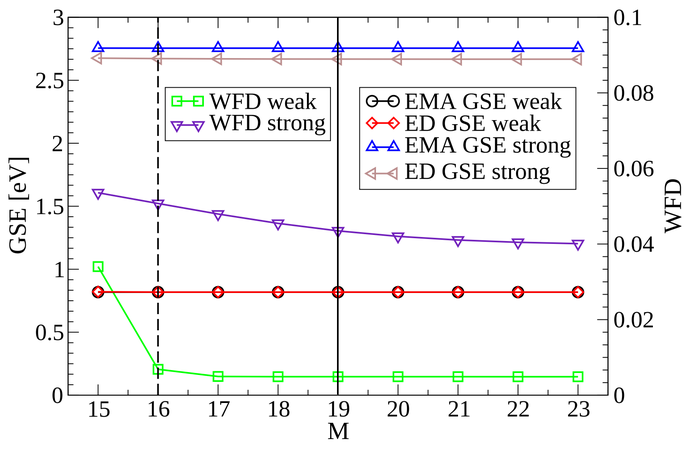

Figure 3: *Plotted are groundstate energies and wavefunction differences (WFD) as a function of the plavewave set $\widetilde{\Gamma}(\Omega)$ from Eq. (12). The solid vertical line and the dashed one indicate the convergence up to a meV for the GSE in the ED and EMA case respectively.*

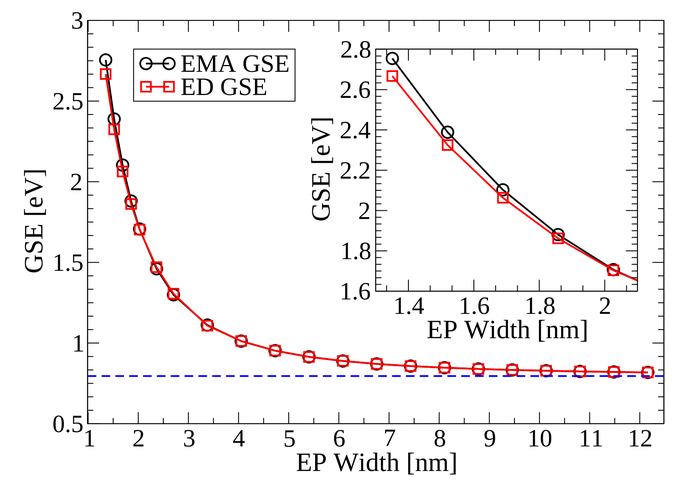

Figure 4: *GSE as a function of the EP width $d = \sqrt{3}Nb$. Below ≈ 2nm the discrepancy between the EMA and the ED results reaches some tenths of an eV. The dashed line shows the edge $E_0 = 0.79$eV from Eq. (8). The difference between the wavefunctions for the two limiting cases $b = 9a_B$ and $b = 1a_B$ can be found in Fig. 3.*